

Multi-objective design and optimization of forklift gantry by using multiple surrogate models

Liye Lv^{1,2}, Baochang Zhu¹, Y. Lu², Y. Mei¹, Yuan Song²

1 Noblelift Intelligent Equipment Co., Ltd., Huzhou, Zhejiang, China, 313000

2 School of Mechanical Engineering, Zhejiang Sci-Tech University, Hangzhou, Zhejiang, China, 310018

Abstract

Forklift is a kind of material handling robot, which is widely used in short-distance handling in the industrial field. However, at present, the structural design of forklifts is generally based on designers' experience, and there are still many problems in domestic forklifts compared with foreign countries. In this paper, the forklift gantry is taken as the research object, and four typical surrogate modeling techniques, namely PRS, KRG, RBF, and SVR models, are used for optimal design and analysis. The study shows that the KRG model has the best performance and RBF model has the worst performance in terms of global and local accuracy. Multi-objective optimization design of the weight and total deformation of the gantry is carried out with the maximum stress of the gantry and I-beam geometry as constraints. Taking the KRG model as an example, the comparison of the results before and after optimization shows that the weight of the I-beam of the forklift gantry is reduced by 11.9% and the maximum total deformation is reduced by 23.2% while satisfying the constraints. Global sensitivity analysis (GSA) of the forklift gantry reveals that the height of the I-beam has the greatest impact on the gantry performance.

OPEN ACCESS

Published: 03/10/2023

Accepted: 06/09/2023

DOI:
10.23967/j.rimni.2023.09.003

Keywords:
Multi-objective Optimization
Surrogate model
Forklift
Gantry

1. Introduction

Industrial vehicles play a crucial role in the national economy and production activities. Industrial vehicles are mainly divided into counterweight forklifts, forward moving forklifts, plug-in forklifts, pallet stackers, pallet handling trucks, bidirectional/multi-directional operation forklifts, etc. They are widely used in ports, stations, airports, freight yards, factory workshops, warehouses, distribution centers, and distribution centers to load, unload, and handle pallet goods in cabins, carriages, and containers. Forklifts experience safety accidents every year causing significant losses. If risks of forklifts can be predicted in advance, most accidents may be avoided. In the past, the design of the forklift was mainly designed and tested in cycles by comparing similar products, i.e., estimating the dimensions of each component based on experience, designing, and installing each component according to drawings, and finally verifying the rigidity and strength. This traditional method can undoubtedly increase the manufacturing cost, and at the same time, due to the large human factor, there will be design deviations and other problems. With the wide application of computer-aided engineering technology, it has brought great convenience to forklift design and solved the above-mentioned problems to a certain extent. However, take the forklift gantry which is the most important part of forklift as an example, computational analysis and design of structural gantry often revolve multiple variables and strong nonlinearity, requiring significant computing cost, and sometimes the most optimal design cannot be found. To mitigate the mathematical and computing cost, surrogate model techniques based on a small amount of sample data is a fast and effective method for structural design, optimization, and analysis.

Up to now, a lot of efforts have been made to apply surrogate models for different optimization design problems of different fields [1], namely mechanical engineering, material, fluid,

architecture, etc. In 2012, Song et al. [2] used single surrogate models to approximate the crash-worthiness optimization of thin-walled structure. In 2019, Asteris et al. [3] proposed a self-compacting concrete strength prediction method by using surrogate model technique. In 2020, Sun et al. [4] considered to ease the cost of numerical simulations on fluid dynamics problems and developed a physics-constrained surrogate model. In 2021, Zhang et al. [5] proposed a multi-fidelity surrogate model-based optimization framework by correlating the configuration parameters of an aircraft and its aerodynamic performance. In 2022, Li et al. [6] offered a vectorial surrogate model-based multi-failure correlated probabilistic evaluation method for evaluating the reliability performance of complex structures, like turbine rotor. In 2023, Yuan et al. [7] used the radial basis function (RBF) model and alpine skiing optimization algorithm [8] to minimize the operating cost of the dynamic positioning system. After studying some recent literature, we found that even though surrogate model techniques have been developed for more than three decades and some classical theories were proposed long ago and are relatively mature, the vitality of surrogate model techniques does not stop and still plays an important role in various fields with continuous theoretical innovations.

Forklift is a type of material handling robot, and industrial robots first originated in the U.S. In 1954, George C. Devol designed the world's first truly robotic arm, which was later bought by Joseph F. Engelberger with related patents, and established the world's first robotics company, namely Unimation, which developed two types of robots, i.e., Versatran and Unimate. Since then, material handling robots have been appearing in factories and workshops. In 1961, Stanford University developed Shakey, an autonomous mobile robot [9]. With the development of computer technology and sensor technology, countries in the United States, Japan, and Europe have begun to work on the development of mobile robots.

Domestic research in this field started late and the technology is relatively weak, however, with the national emphasis on robotics industry and the continuous progress of science and technology, the development has been very rapid in recent decades, and many universities, research institutes and enterprises (such as Xinsong, CSG Huaxiao, Jizhijia, NOBLELIFT, etc.) have also actively invested in the research of robotics industry. The first fully hydraulic heavy-duty handling robot in China was developed by Qingdao Huadong Construction Machinery Co., Ltd. and the TPR series robots were developed by the Robotics Research Institute of Shanghai Jiaotong University in cooperation with Wadi Packaging Technology Co. As the largest robot company in China, mobile robots are one of the most internationally competitive products of Xinsong. The first AGV of Xinsong was applied in the automotive industry and exported to Mexico and the U.S., laying the foundation for the domestic material handling robots to the international market. CSG Huaxiao is a wholly-owned subsidiary of KDDI, which has been cultivating in the field of intelligent material handling equipment for nearly forty years and holds many core technologies and patents of intelligent handling.

Overall, compared with the advanced level of international material handling robots, domestic material handling mobile robot research is still in its infancy, in material handling accuracy, speed, reliability, load-bearing capacity, design level and other aspects there is still a large gap, the relevant core technology industrialization and localization still exists a large shortage, in addition to some key components still rely on imports. However, with the research and application of new technologies, the transformation and upgrading of the manufacturing industry and the urgent demand for manpower replacement, the application prospect of material handling mobile robots is very wide in the context of the development of intelligent workshops, and how to develop unmanned handling robots that can meet the needs of users in all aspects is a realistic problem that must be faced in the future.

Forklifts are wheeled handling vehicles for loading, unloading, stacking, and transporting goods over short distances. As one of the most typical industrial transporting vehicles, forklifts have been widely used in ports, stations, airports, yards, factory floors, warehouses, and other sectors of the national economy for their high productivity, low operating costs, high operational safety, and low cargo losses. The gantry is one of the key components of forklifts. It is generally composed of inner and outer gantry, fork frames, forks, lifting oil tanks, tilting oil tanks, chains, oil pipes, roller bearings and other structural components. The gantry plays the role of rising and falling in the forklift lifting mechanism, which is the basis for the operation of the gantry system. When lifting the cargo, it is supported by a lifting cylinder to withstand the axial force of the cargo. At the same time, the weight of the cargo acts on the fork, which is transmitted to the gantry through the fork frame, so that the gantry bears the bending moment. Therefore, the inner and outer gantries of the forklift play a crucial role in the gantry system of the forklift.

The early investigations of forklift gantry were concentrated on the reducing shock of gantry using MATLAB optimization toolbox, decreasing noise through the optimization of cross-sectional selection of the gantry steel. Previous researchers mostly based on the strength analysis and verification of the gantry system, starting from structural optimization and verification, but there is still a certain gap between the real application of various research results to the mass production of products. This paper put pressure on optimization design and analysis of the forklift gantry by using multiple surrogate models. Surrogate models have been significantly improved over the past three decades, and many kinds of surrogate

models such as polynomial regression surface (PRS) [10], Kriging (KRG) [11], radial basis function (RBF) [12], and support vector regression (SVR) [13], have been developed and successfully applied in many structure and/or multidisciplinary design optimization problems. However, different kinds of surrogate models often have different modeling precision, design and analysis results due to their own mathematical characteristics. That is, without sufficient prior information, it is often unknown which surrogate model performs best for the same problem. Therefore, in this paper, considering the uncertainty of the approximation model prediction, we tried different kinds of surrogate models for the design and analysis of the gantry, and selected the most suitable model from them based on the estimation of various errors.

The rest of this paper is organized as follows. The forklift and forklift gantry are introduced briefly in Section 2, and Section 3 focuses on surrogate models approximating the gantry. Section 4 compares the performance of four individual surrogate models, and then surrogate-based design and optimization for the gantry is implemented. Conclusions and future work are provided in Section 5.

2. Numerical analysis of forklift gantry

2.1 Introduction of forklift

Forklifts are battery-powered industrial vehicles, usually equipped with electromagnetic or optical automatic guidance devices, can be under the control of the control system, according to the established path planning, accurately move to the designated location, complete a series of work tasks. Forklift is generally composed of mechanical system, power system and control system, which is the product of multidisciplinary integration of mechanical engineering, computer engineering, control engineering and artificial intelligence, etc. With the development of information technology and automation technology, forklifts are also widely used in various fields such as handling, stacking, and logistics, etc. The configuration of a forklift is shown in [Figure 1](#). The forklift consists of forklift body, gantry system, lifting platform, docking mechanism, and hydraulic system. The gantry system is installed on the forklift body and is used to lift the platform, which can move up and down under the guidance of the gantry system. The front end of the lifting platform is equipped with a secondary docking mechanism, and the secondary docking mechanism has a hydraulic system that can control the movement of the secondary docking mechanism.

2.2 Gantry structure

The gantry system consists of two lifting rails, lower cross member plate, middle cross member plate, upper cross member plate, lifting hydraulic cylinder and U-shaped sprocket frame, as shown in [Figure 2\(a\)](#). The two ends of the lower crossbeam, middle crossbeam, and upper crossbeam are fixed to the lifting rail, and the rear end of the middle crossbeam is provided with a rear tubing clamp. The critical component of gantry system is gantry as shown in [Figure 2\(b\)](#). As an important working device of forklift, the rationality of its lifting system design directly determines the quality of forklift. In daily operation, the gantry will be subjected to relatively complex forces in repeated lifting operations. Therefore, the structural design and optimization of gantry will directly lead to the degree of deformation of each component and the failure of the structure, which affects the safety performance, work efficiency and other related functions of the gantry system, and then seriously affects the life of each system of the forklift truck.

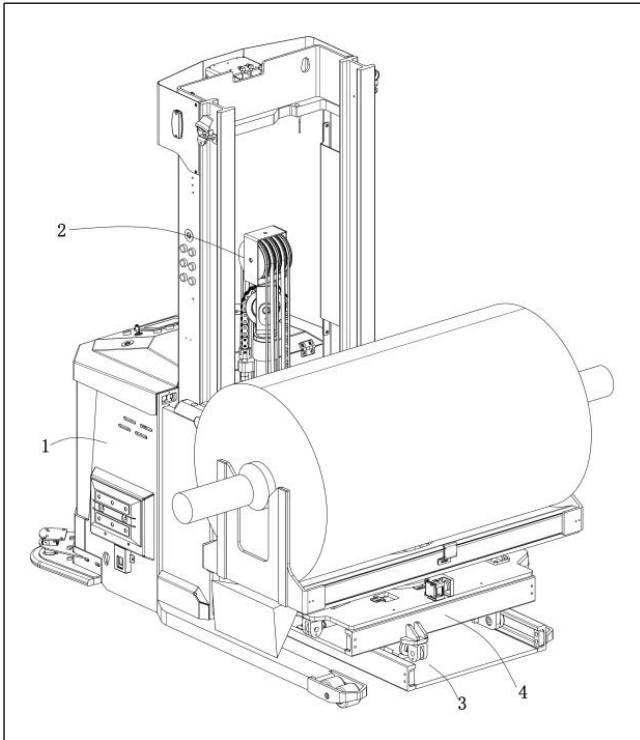
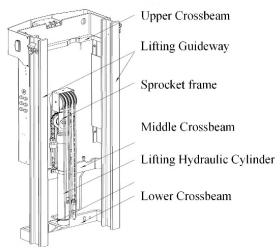
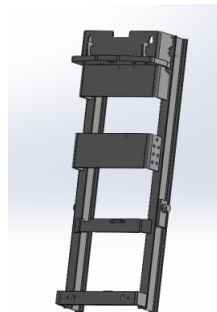


Figure 1. Structural diagram of AGV (1-forklift body, 2-lifting system, 3-lifting platform, 4-docking mechanism)



(a) Gantry system



(b) Gantry

Figure 2. Structural diagram of gantry

2.3 Gantry simulation analysis

The three-dimensional (3-D) model of the gantry was created using SolidWorks, and the parts such as forks, gantry, lifting chain, sprockets, lifting hydraulic cylinder and tilting cylinder were created in turn according to the actual dimensions. Here we mainly focus on the design, optimization, and analysis of the gantry. The 3-D model of gantry is imported into ANSYS Workbench for static analysis. The material of the gantry is 25MnV alloy steel with the following material parameters: density of 7850 kg/m³, modulus of elasticity of 2.06*10⁵ MPa, and Poisson's ratio of 0.3.

As the main structure of the gantry, I-beam is an important structure to support the gantry and transfer the force on the

gantry, and its strength also determines whether the forklift can complete the engineering transportation work more efficiently and safely. Therefore, structural optimization of I-beams can further reduce stress and deformation, reduce mass, and improve the economy and overall stability while ensuring the strength. Four design variables are selected to design and optimize the I-beam section, as shown in Figure 3(a), namely the height of I-beam h , the width of I-beam b , the waist thickness of I-beam d , and average thickness of I-beam t .

The gantry is free-grid with a grid cell size of 10 mm and the stress concentration region is locally encrypted, yielding a total of 111,777 grid cells and 223,976 nodes. The main loads and restraints on the gantry include the fixed restraint at the bottom of the gantry, which restricts the displacement of the gantry; the downward pressure F acting on the top of the I-beam; and the moment M generated by the downward translational pressure from the forks with a full load of 2 tons; also, the gravity of the gantry itself, G . The overall load diagram of the gantry is shown in Figure 3(b).

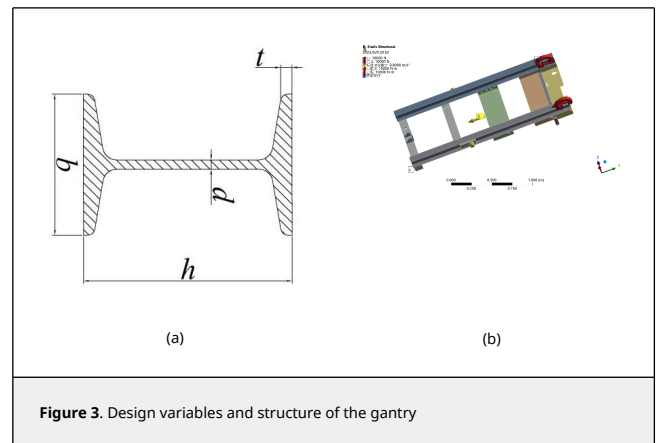


Figure 3. Design variables and structure of the gantry

3. Design and optimization with multiple surrogate models

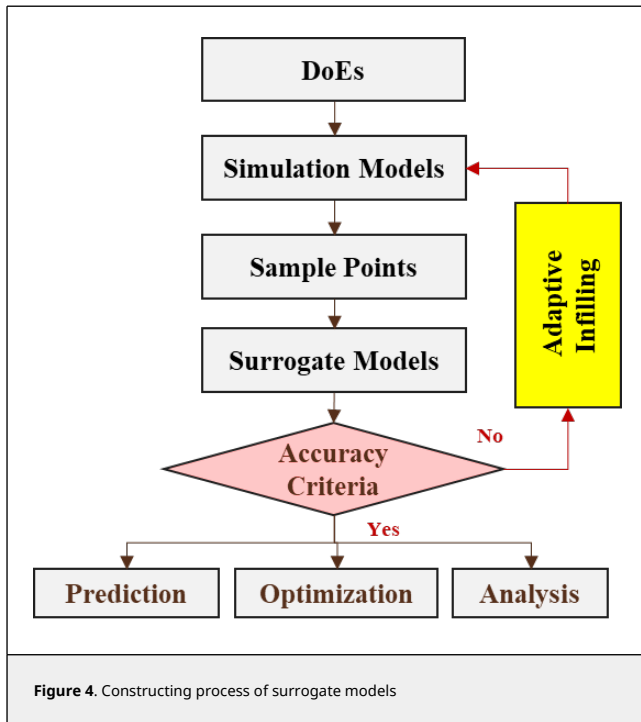
3.1 Surrogate models

The surrogate model is an approximate mathematical model widely used in engineering design and optimization problems to replace more complex and time-consuming numerical analysis, and the relationship between the input parameter variable and the output objective function of the system can be fitted on the basis of fewer sample points in the design space of complex systems [10], which has the characteristics of good fitting accuracy, low cost and high work efficiency.

The typical constructing process of surrogate models is shown in Figure 4, which mainly includes design of experiments (DoEs), generation of sampling points, construction of surrogate models, accuracy evaluation and application. If the accuracy of surrogate models cannot meet the requirements of the accuracy criteria, new sampling points generated by adaptive infilling method should be added into the initial sample set. Four typical individual surrogate models are briefly introduced next, and relevant theory is detailed in references [7-10].

3.1.1 PRS

PRS is a regression model with good global approximation performance, poor local performance, simple form, and good transparency. Although PRS can be used to fit linear or nonlinear problems, its resistance to interference and local



fitting ability are poor when the problem has a large number of design variables and a high degree of nonlinearity. Therefore, PRS is mainly applied to low-dimensional and low-nonlinear problems. In practice, first-order or second-order PRS is usually used, and here second-order PRS is taken as example in Eq. (1)

$$\hat{y} = \omega_0 + \sum_{i=1}^n \omega_i x_i + \sum_{i=1}^{n-1} \sum_{j=i+1}^n \omega_{ij} x_i x_j + \sum_{i=1}^n \omega_{ii} x_i^2 \quad (1)$$

where \hat{y} is the prediction at unknown point x , ω denotes the fitted weight coefficient which is evaluated by using sampling points, and n expresses the number of variables.

3.1.2 KRG

The KRG model is essentially a linear weighted combination of information from known points to predict unknown information within a certain range. Unlike the PRS model, the KRG model has good local estimation capability because of the correlation functions, good continuity and derivability, and good approximation for nonlinear complex problems. General form of the KRG model can be expressed as

$$\hat{y} = \hat{\mu} + \mathbf{r} \mathbf{R}^{-1} (\mathbf{y} - 1 \hat{\mu}) \quad (2)$$

where \mathbf{y} is the true response vector at sampling points, \mathbf{R} is the correlation matrix of known sampling points, and \mathbf{r} denotes the correlation vector between the unknown point and known sampling points, and $\hat{\mu}$ is the evaluated mean. Generally, the kernel function used in the KRG model is the Gaussian function (see Simpson et al. [11] for details).

3.1.3 RBF

The RBF method uses basis functions to transform a high-dimensional nonlinear problem into a low-dimensional linear weighted problem, where the basis functions used are radially symmetric functions centered on the sampling points. The RBF

model has been widely used because of its strong robustness and adaptability, as well as its fast convergence and low computational cost, and its ability to fit many types of functions very well. The basic mathematical expression of the RBF model is

$$\hat{y} = \omega^T \mathbf{r} = \sum_{i=1}^n \omega_i r_i (\| \mathbf{x} - \mathbf{x}_i \|) \quad (3)$$

where \mathbf{x}_i which is the i -th sampling point, is also the i -th center point of the basis function, \mathbf{r} denotes the correlation between the unknown point and the n sampling points. The weight coefficient vector ω can be evaluated according to the known points (see Matheron [12] for details).

3.1.4 SVR

SVR model is a specific implementation of support vector machine (SVM). The essence of the SVR model is to implement linear support vector machine regression in high-dimensional space by nonlinearly mapping low-dimensional data to high-dimensional space through kernel functions. Compared to the first three models, the SVR model is more flexible and can be used in areas such as financial market forecasting [14] and probabilistic stability analysis [15]. The linear regression formula for SVR can be expressed as

$$\hat{y} = \sum_{i=1}^n (\alpha_i - \alpha_i^*) (\mathbf{x}_i \cdot \mathbf{x}) + b \quad (4)$$

where α_i and α_i^* are dual variables, and b is the base term (see Clarke et al. [13] for details).

3.2 DoEs

According to the construction process of the surrogate model in Figure 5, the range of design variables was determined after analyzing the problem, and DoEs can be performed using sampling methods. There are several typical sampling methods, such as Latin hypercube sampling (LHS) [16], full factorial design (FFD) [17], orthogonal array (OA) [18], and central composite design (CCD) [19] methods. In this paper, the LHS method was used to generate training and testing samples in the design space. 50 points were selected and the corresponding maximum stress and maximum total deformation under the relevant loads were calculated using simulation. The 50 points are divided into two groups, 40 points are used for training surrogate models and the remaining 10 points are used for testing the built surrogate models. 40 training points and 10 testing points are illustrated in Figure 5. In Figure 5, h , b , t , and d are design variables shown in Figure 3(a). It can be clearly seen that the training and testing points are distributed over almost the whole design space with good space filling property and projection. The testing points and training points are in the same design space, which does not involve the problem of external interpolation, while the testing points and training points are interspersed with each other, indicating that distribution of sampling points can meet the requirements.

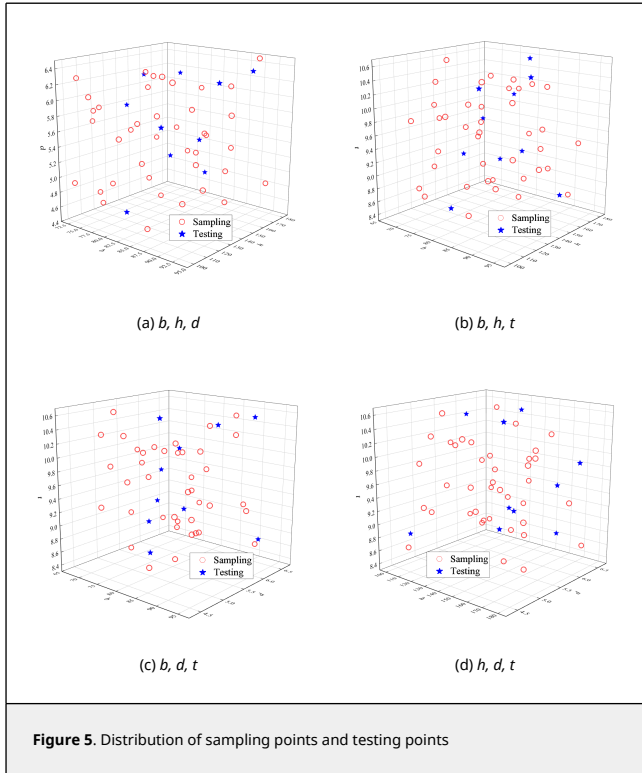


Figure 5. Distribution of sampling points and testing points

3.3 Accuracy evaluation methods

When a surrogate model is established, we need to test the accuracy of the model to determine the fit of the model, and only the surrogate model with qualified accuracy can meet the requirements of engineering applications. A common method is to compare the calculated or simulated response values of another set of test points with the predicted response values of the surrogate model. The commonly used determination criteria are multiple Coefficient of determination R^2 (R -square), normalized root mean squared error ($NRMSE$) and normalized maximum error ($NMAE$) which are calculated as follows

$$R^2 = 1 - \frac{\sum_{i=1}^{nt} (y_i - \hat{y}_i)^2}{\sum_{i=1}^{nt} (y_i - \bar{y})^2} \quad (5)$$

$$NRMSE = \sqrt{\frac{\sum_{i=1}^{nt} (y_i - \hat{y}_i)^2}{\sum_{i=1}^{nt} y_i^2}} \quad (6)$$

$$NMAE = \max \left(\frac{|y_i - \hat{y}_i|}{\sum_{i=1}^{nt} (y_i - \hat{y}_i)^2} \right) \quad (7)$$

where nt is the number of testing points, y_i and \hat{y}_i are the true response and the prediction of the surrogate model at the testing point x_i , respectively. From the above equations, we can

see that the value of R^2 is between 0 and 1, the closer the value of R^2 is to 1, the closer the surrogate model is to the real situation, namely the higher the global accuracy. The value of $NRMSE$ is greater than 0, depending on the system response amplitude, the smaller the value of $NRMSE$ for the same response surface, the higher the global accuracy of the surrogate model. Similar to $NRMSE$, the value of $NMAE$ is greater than 0, the smaller the value of $NMAE$ for the same response surface, the higher the local accuracy of the surrogate model.

4. Results

4.1 Accuracy analysis of surrogate models

In order to explore the performance of different individual surrogate models intuitively, both global criteria (i.e., R^2 and $NRMSE$) and local criterion (i.e., $NMAE$) are employed which are displayed by bar charts in Figure 6 and listed in Table 1. It is obvious that the four surrogate models can better approximate the total deformation and maximum stress. For the gantry weight, the formula can usually be established with the given four design variables, so surrogate models can fit the gantry weight well. However, the fitting accuracy of the RBF model for the gantry weight is poor, probably due to the overfitting during the fitting process, which leads to a sharp decrease in the global fitting accuracy. In addition, it is found that surrogate models with better global accuracy do not necessarily have the best local accuracy, as in Figure 6(a), the global accuracy of PRS, KRG, and SVR are better than that of RBF, but the local accuracy of RBF model is better than that of the other three surrogate models. Considering the global and local performance together, for total deformation, maximum stress, and weight of gantry, the KRG model performs best, followed by the PRS model and the SVR model, and finally by the RBF model.

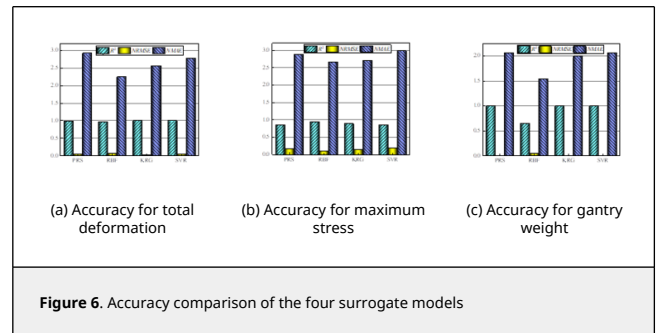


Figure 6. Accuracy comparison of the four surrogate models

Table 1. Accuracy evaluation of the four surrogate models

Response	Criteria	PRS	RBF	KRG	SVR
Total Deformation	R^2	0.99	0.96	1.00	0.99
	$NRMSE$	0.04	0.07	0.02	0.04
	$NMAE$	2.90	2.24	2.55	2.77
Maximum Stress	R^2	0.86	0.94	0.89	0.85
	$NRMSE$	0.18	0.12	0.16	0.18
	$NMAE$	2.87	2.65	2.70	2.97
Gantry Weight	R^2	1.00	0.65	0.99	1.00
	$NRMSE$	0.01	0.06	0.01	0.00
	$NMAE$	2.05	1.54	1.99	2.06

4.2 Optimization and analysis

4.2.1 Problem definition

The surrogate models built in Section 3 need to be used instead of the simulation model for optimization design and analysis. In the whole gantry optimization process, total deformation and

gantry weight are the two optimization objectives. In fact, these two optimization goals are contradictory to each other. Structures with less deformation have better rigidity and corresponding weight will be larger. Therefore, this problem is a multi-objective optimization design problem. There are two main constraints. The first one is the maximum stress. The material of the gantry is 25 MnV alloy steel with yield strength of 590.0 MPa, and the safety factor is taken as 1.8, then the allowable stress of the gantry is $[\sigma] = \frac{590}{1.8} = 327.8$ MPa, and the maximum stress of the gantry $\sigma_{\max} \leq [\sigma]$. The other one is the gantry size. Considering the specific applications and working conditions, load, and local stability, it is necessary to constrain geometry size of the non-standard I-beam. To obtain the optimal design of the forklift gantry, multi-objective generic algorithm (MOGA) is used herein. The entire gantry optimization problem is then described as Eq. (8). To obtain the optimal design of the forklift gantry, generic algorithm (GA) is used herein

$$\begin{aligned} \min \quad & F(b, h, d, t) = \omega_1 f_1 + \omega_2 f_2 \quad (8) \\ \text{s.t.} \quad & \sigma_{\max} \leq 327.8 \\ & 68.0 \leq b \leq 94.0 \\ & 100.0 \leq h \leq 180.0 \\ & 4.5 \leq d \leq 6.5 \\ & 8.4 \leq t \leq 10.8 \end{aligned}$$

where $F(\cdot)$ is the total objective, f_1 means the total deformation, f_2 is the gantry weight, ω_1 and ω_2 are coefficient weights of two objectives, respectively, and the sum of these two is 1.

It should be noted that due to the different dimensions and orders of magnitude of the two optimization objectives, they are normalized and then subjected to linear weighted multi-objective optimization. Hence, D means the normalized total deformation, and M means the normalized the gantry weight. According to the experience, total deformation of the forklift gantry is more important than the gantry weight, so ω_1 is set to be larger than and equal to ω_2 . Three different values of ω_1 , namely 0.5, 0.6, and 0.7, were selected and the predicted and true responses of the objective function and constraints were compared. Results are listed in Tables 2, 3, and 4. From the optimization results based on surrogate models, coefficient weight has a certain influence on the optimization results, and the best results are obtained when ω_1 is equal to 0.6. Therefore, it is appropriate to take ω_1 equal to 0.6 and ω_2 equal to 0.4.

Table 2. Comparison of optimization results of the four surrogate models for $\omega_1=0.5$

Response	b (mm)	h (mm)	d (mm)	t (mm)	Total Deformation (mm)	Maximum Stress (MPa)	Gantry Weight (Kg)	
Before optimization	81.0	140.0	5.5	9.6	10.8	317.0	35.9	
After optimization	PRS	68.4	169.4	4.5	8.4	8.7	220.6	30.8
	RBF	68.0	169.1	4.5	8.4	8.5	285.9	31.2
	KRG	69.1	171.0	4.5	8.4	8.4	267.9	30.7
	SVR	68.9	167.9	4.5	8.5	8.8	246.4	30.9

Table 3. Comparison of optimization results of the four surrogate models for $\omega_1=0.6$

Response	b (mm)	h (mm)	d (mm)	t (mm)	Total Deformation (mm)	Maximum Stress (MPa)	Gantry Weight (Kg)	
Before optimization	81.0	140.0	5.5	9.6	10.8	317.0	35.9	
After optimization	PRS	68.1	170.2	4.5	8.4	8.6	218.3	30.8
	RBF	68.8	169.5	4.6	8.4	8.4	281.1	31.4
	KRG	68.1	179.3	4.5	8.4	7.7	239.9	31.2
	SVR	72.5	178.2	4.6	8.4	7.5	253.1	32.6

Table 4. Comparison of optimization results of the four surrogate models for $\omega_1=0.7$

Response	b (mm)	h (mm)	d (mm)	t (mm)	Total Deformation (mm)	Maximum Stress (MPa)	Gantry Weight (Kg)	
Before optimization	81.0	140.0	5.5	9.6	10.8	317.0	35.9	
After optimization	PRS	70.1	178.4	4.9	8.4	7.4	234.3	32.6
	RBF	69.4	170.4	4.5	8.4	8.2	275.5	31.6
	KRG	68.1	180.0	4.5	8.4	7.6	236.8	31.2
	SVR	68.6	173.8	4.8	8.5	7.9	261.8	31.8

In order to check the accuracy of the optimization results obtained from the four surrogate models, they were substituted into the simulation model to obtain the real results as listed in Tables 5, 6, and 7. Tables 5, 6, and 7 list the total deformation, maximum stress, and gantry weight results of before and after optimization based on the four surrogate models, respectively. From the results of after optimization, the errors of total deformation of the PRS, RBF, KRG, and SVR model are 3.6%, 2.4%, 1.3%, and 1.4%, respectively. The errors of maximum stress of the PRS, RBF, KRG, and SVR model are 16.5%, 9.5%, 4.4%, and 1.4%, respectively. The errors of the I-beam weight of the PRS, RBF, KRG, and SVR model are 0.6%, 0.0%, 1.6%, and 1.5%, respectively. Collectively, the SVR model performs the best, followed by the KRG model, and the accuracy of PRS and RBF model is similar, which is similar to the results obtained in Section 4.1.

From the comparison of before and after optimization, for the total deformation, PRS, RBF, KRG, and SVR model decreases 16.2%, 17.2%, 23.2%, and 25.3%, respectively. For the maximum stress, PRS, RBF, KRG, and SVR model decreases 17.1%, 18.6%, 20.4%, and 20.8%, respectively. For the I-beam weight, PRS, RBF, KRG, and SVR model decreases 14.9%, 12.8%, 11.9%, and 8.1%, respectively. The comparison shows that the optimal design based on KRG model has the best performance. Hence, the optimal solution obtained from the KRG model was substituted into the simulation model and a comparison of the results before and after optimization was shown in Figures 7 and 8.

Table 5. Total deformation results of before and after optimization

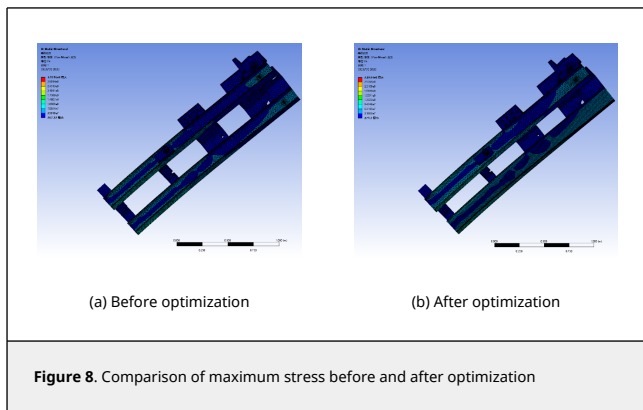
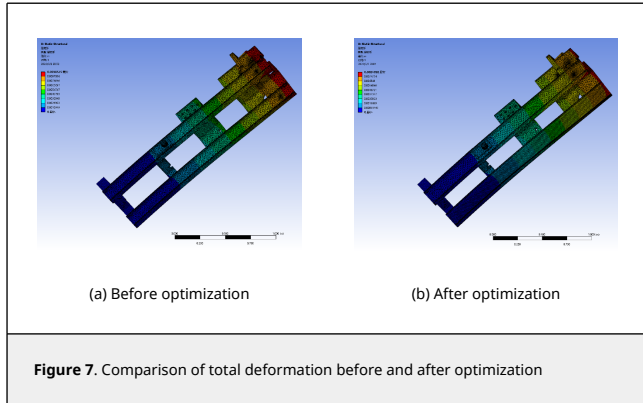
Optimal model	After optimization			Before optimization	Decrease
	Prediction	True	Error		
PRS	8.6	8.3	3.6%	9.9	16.2%
RBF	8.4	8.2	2.4%	9.9	17.2%
KRG	7.7	7.6	1.3%	9.9	23.2%
SVR	7.5	7.4	1.4%	9.9	25.3%

Table 6. Maximum stress results of before and after optimization

Optimal model	After optimization			Before optimization	Decrease
	Prediction	True	Error		
PRS	218.3	261.3	16.5%	315.2	17.1%
RBF	281.1	256.6	9.5%	315.2	18.6%
KRG	239.9	250.9	4.4%	315.2	20.4%
SVR	253.1	249.7	1.4%	315.2	20.8%

Table 7. Maximum stress results of before and after optimization

Optimal model	After optimization			Before optimization	Decrease
	Prediction	True	Error		
PRS	30.8	31.0	0.6%	36.0	14.9%
RBF	31.4	31.4	0.0%	36.0	12.8%
KRG	31.2	31.7	1.6%	36.0	11.9%
SVR	32.6	33.1	1.5%	36.0	8.1%



4.2.2 Global sensitivity analysis

Global Sensitivity analysis (GSA) is to study the impact of simultaneous changes of different input parameters on the system or model in the entire design space. The most representative Sobol's GSA method [20] is used in this study, which is a sensitivity analysis method based on variance. This method can simultaneously calculate the first order sensitivity index and the full order sensitivity index of design variables, where the first order sensitivity represents the influence of a single design variable, while the full order sensitivity considers the interaction between each variable. Given any integrable function in n -dimensional space, it can be represented as

$$f(x) = f_0 + \sum_i f_i(x_i) + \sum_{i < j} f_{ij}(x_i, x_j) + f_{12...n}(x_1, x_2, \dots, x_n) \quad (9)$$

where x_i and x_j are the i -th and j -th variables, respectively.

The total variance and partial deviation of $f(x)$ are shown in Eqs. (10) and (11)

$$D = \int f^2(x) dx - f_0^2 \quad \text{QUOTE } D = \int f^2(x) dx - f_0^2 D = \int f^2(x) dx - f_0^2 \quad (10)$$

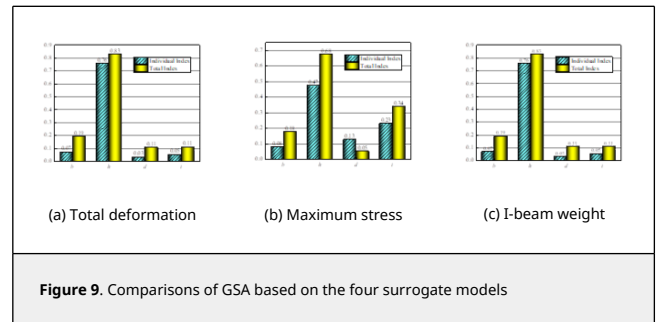
$$D_{i_1...i_s} = \int f_{i_1...i_s}^2(x) dx_{i_1} \dots dx_{i_s} \quad D_{i_1...i_s} = \int f_{i_1...i_s}^2(x) dx_{i_1} \dots dx_{i_s} \quad (11)$$

The first-order sensitivity index of each variable is as follows

$$S_i = \frac{D_{i_1...i_s}}{D} \quad (12)$$

where S_i denotes the first-order sensitivity index of the i -th variable. The full-order sensitivity index $S_{i_1...i_s}$ of the i -th variable is the sum of the sensitivity indices of the i -th variable.

The GSA of the gantry is carried out based on the four surrogate model, and results are shown in Figure 9. It is obvious that the height of I-beam h has the greatest impact on the total deformation, maximum stress, and the I-beam weight, with the highest first-order sensitivity index and full-order sensitivity index, which are greater than the total influence of the other 3 variables. From Figure 9(b), the average thickness of I-beam t also affects the maximum stress of the gantry to some extent. The other two parameters, namely b and d , have almost negligible effects on the total deformation, maximum stresses, and I-beam weight.



When designing the gantry, great attention should be paid to the influence of the height of I-beam. Compared with the simulation-based GSA, the surrogate-based GSA method can save a lot of time. In this problem, using 10000 Monte Carlo sample points, it needs to build a model 20000 times, and it takes about 48 hours to run the Sobol's GSA method once, while it takes about 30 minutes to run the gantry model once, and it takes about 10000 hours to run 20000 times, which increases the speed by about 2083 times. The surrogate model technique has proven to be more effective for GSA method and more suitable for GSA of mechanical equipment and systems.

5. Conclusions

This paper reviewed the previous gantry optimization design methods and surrogate models in different fields, as well as the development history of forklift industrial robots. Due to the gap between the domestic forklift research in terms of scientific application and product production, this paper compares and studies the application of four surrogate models, namely PRS, KRG, RBF and SVR, in the multi-objective optimization design of forklift gantry. The main conclusions are as follows.

1) The 3-D model of the gantry was established through statistical analysis and numerical settings, and four parameters, namely height h , width b , waist thickness d , and average thickness t of the I-beam were selected as the design variables. Using the LHS sampling method, 40 training points and 10 testing points with good projection and space-filling property were selected.

2) Global accuracy criteria (R^2 and $NRMSE$) and local criterion (NMAE) were used to evaluate the prediction accuracy of each surrogate model. Comparing the total deformation, maximum stress, and I-beam weight, the KRG model performed the best, followed by the PRS model and the SVR model, and finally by the

RBF model.

3) Multi-objective optimization design for maximum total deformation and I-beam weight was conducted using I-beam geometry and maximum stress as constraints. Results of before and after optimization show that, for the total deformation, PRS, RBF, KRG, and SVR model decreases 16.2%, 17.2%, 23.2%, and 25.3%, respectively. For the maximum stress, PRS, RBF, KRG, and SVR model decreases 17.1%, 18.6%, 20.4%, and 20.8%, respectively. For the I-beam weight, PRS, RBF, KRG, and SVR model decreases 14.9%, 12.8%, 11.9%, and 8.1%, respectively. The optimal design based on KRG model has the best performance.

4) Finally, using the KRG model and Sobel's GSA method, the GSA of the gantry was investigated. The height of the I-beam has the greatest influence on the performance of the gantry, and the average thickness also has a certain influence on the maximum stress of the gantry, so it is necessary to pay more attention to the height of the I-beam and the average thickness of the I-beam when designing forklift gantries in the future.

Acknowledgment

The research was supported by the Zhejiang Province Key Research and Development Project (2021C01070) and Zhejiang Province Science and Technology Plan Project (2023C01174).

Data availability statement

The data that support the findings of this study are available from the corresponding author upon reasonable request.

References

- [1] Yuan Y., Mu X., Shao X., Ren J., Zhao Y., Wang Z. Optimization of an auto drum fashioned brake using the elite opposition-based learning and chaotic k-best gravitational search strategy based grey wolf optimizer algorithm. *Applied Soft Computing*, 123, 108947, 2022.
- [2] Song X., Sun G., Li G., Gao W., Li Q. Crashworthiness optimization of foam-filled tapered thin-walled structure using multiple surrogate models. *Structural and Multidisciplinary Optimization*, 47(2):221-231, 2013.
- [3] Asteris P.G., Ashrafian A., Rezaie-Balf M. Prediction of the compressive strength of self-compacting concrete using surrogate models. *Computers and Concrete*, 24(2):137-150, 2019.
- [4] Sun L., Gao H., Pan S., Wang J.X. Surrogate modeling for fluid flows based on physics-constrained deep learning without simulation data. *Computer Methods in Applied Mechanics and Engineering*, 361:1-25, 112732, 2020.
- [5] Zhang X., Xie F., Ji T., Zhu Z., Zheng Y. Multi-fidelity deep neural network surrogate model for aerodynamic shape optimization. *Computer Methods in Applied Mechanics and Engineering*, 373, 113485, 2021.
- [6] Shanahan M. Shakey and the turtle: cognitive robotics finds biological inspiration. *EPSCRBBSRC International Workshop, Biologically Inspired Robotics: Legacy of W. Grey Walter*, pp. 256-263, 2002.
- [7] Yuan Y., Shen Q., Xi W., Wang S., Ren J., Yu J., Yang Q. Multidisciplinary design optimization of dynamic positioning system for semi-submersible platform. *Ocean Engineering*, 285, 115426, 2023.
- [8] Yuan Y., Ren J., Wang S., Wang Z., Mu X., Zhao W. Alpine skiing optimization: A new bio-inspired optimization algorithm. *Advances in Engineering Software*, 170, 103158, 2022.
- [9] Li X.Q., Song L.K., Bai G.C. Vectorial surrogate modeling approach for multi-failure correlated probabilistic evaluation of turbine rotor. *Engineering with Computers*, 39(3):1885-1904, 2022.
- [10] Glaz B., Goel T., Liu L., Friedmann P.P., Haftka R.T. Multiple-surrogate approach to helicopter rotor blade vibration reduction. *AIAA Journal*, 47(1):71-282, 2009.
- [11] Simpson T.W., Mauery T.M., Korte J.J., Mistree F. Kriging models for global approximation in simulation-based multidisciplinary design optimization. *AIAA Journal*, 39(12):2233-2241, 2001.
- [12] Matheron G. Principles of geostatistics. *Economic Geology*, 58(8):246-266, 1963.
- [13] Clarke S.M., Griebisch J.H., Simpson T.W. Analysis of support vector regression for approximation of complex engineering analyses. *Journal of Mechanical Design*, 127(6):1077-1087, 2005.
- [14] Kazem A., Sharifi E., Hussain F.K., Saberi M., Hussain O.K. Support vector regression with chaos-based firefly algorithm for stock market price forecasting. *Applied Soft Computing*, 13(2):947-958, 2013.
- [15] Kang F., Li J. Artificial bee colony algorithm optimized support vector regression for

system reliability analysis of slopes. *Journal of Computing in Civil Engineering*, 30(3):04015040, 2016.

[16] Viana F.A.C. A tutorial on Latin hypercube design of experiments. *Quality and Reliability Engineering International*, 32(5):1975-1985, 2016.

[17] Simpson T.W., Poplinski J.D., Koch P.N., Allen J.K. Metamodels for computer-based engineering design: survey and recommendations. *Engineering With Computers*, 17(2):129-150, 2001.

[18] Hedayat A.S., Sloane N.J.A., Stufken J. Orthogonal array: theory and applications. *Technometrics*, 42(4):440-440, 2000.

[19] Tiefang L., Chunlei Z., Guangsheng Y., Jiangsheng W., Guosheng X., Hanlai Z., Yin C., Liu T. Central composite design-based analysis of specific leaf area and related agronomic factors in cultivars of rapeseed (*Brassica napus* L.). *Field Crops Research*, 111(1-2):92-96, 2009.

[20] Sobolá I.M. Global sensitivity indices for nonlinear mathematical models and their Monte Carlo estimates. *Mathematics & Computers in Simulation*, 55(1-3):271-280, 2001.